Наносистеми, наноматеріали, нанотехнології
Nanosistemi, Nanomateriali, Nanotehnologii
2021, т. 19, № 2, сс. 273–280

PACS numbers: 66.30.Pa, 68.43.Bc, 71.15.Dx, 71.15.Mb, 71.20.Tx, 73.20.At, 73.21.Ac

The Comparison of Intercalation of Na and Li Atoms in Nanostructured SnS_2 Anode of Battery: *ab initio* Calculation

Yu. Prikhozha and R. Balabai

Kryvyi Rih State Pedagogical University,
54 Gagarin Ave.,
UA-50086 Kryvyi Rih, Ukraine

Applying the methods of the electron-density functional and *ab initio* pseudopotential, the computational experiment is carried out, using the author's software complex on atomic models that correctly reproduced the 2*D*-layer structure of tin chalcogenides with intercalated Na and Li atoms. We obtain the spatial distributions of the valence electrons' density, the energy reliefs of migration of the Na and Li atoms in the nanostructured SnS_2 interlayer under various degrees of filling of the interlayers with metal atoms. As established, the motion of the Na and Li atoms is accompanied by the overcoming of energy barriers. Barriers depend on the degree of filling of the nanostructured SnS_2 interlayer with metal atoms. The optimum filling of the SnS_2 interlayer with the Na and Li atoms in percentage of 75% is determined, at which the motion of the Na and Li atoms is accompanied by the least energy losses. The processes occurring inside the SnS_2 layer during the migration of the Na and Li atoms are determined by the interaction of metal atoms with each other, which are filling the layer, as well as by the interactions of the Na and Li atoms with a surface SnS_2 layer consisting of sulphur atoms. The distributions of the valence electrons' density, the energy barriers for migration of the Na and Li atoms in the intermediate SnS_2 layer are compared.

Методами функціоналу електронної густини та псевдопотенціялу із перших принципів, з використанням авторського програмного комплексу, що адекватно відтворює шарувату структуру халькогенідів Стануму з інтеркальваними атомами Na та Li, виконано обчислювальний експеримент. Одержано просторові розподіли електронної густини валентних електронів та перетини їх, енергетичні бар'єри міґрації атомів Na та Li в міжшаровому прошарку аноди акумулятора, виконаної з нанорозмірного SnS_2 за різних ступенів наповнености її атомами металу. Проаналізовано рух атомів Na та Li, що супроводжувався доланням енергетичних бар'єрів, величини яких залежали від ступеня наповненості наноструктурного прошарку SnS_2 атомами металу. Зафіксовано оптима-

льну наповненість наноструктурного прошарку SnS_2 атомами Na та Li в 75%, за якої рух атомів Na та Li супроводжувався найменшими енергетичними затратами.

Key words: anode of battery, Na and Li atoms, nanostructured SnS_2 films, electron density functional, *ab initio* pseudopotential, energy reliefs of migration.

Ключові слова: анода акумулятора, атоми Na та Li, наноструктуровані плівки SnS_2, функціонал електронної густини, псевдопотенціял із перших принципів, енергетичні рельєфи міґрації.

(Received 2 June, 2020)

1. INTRODUCTION

Lithium-ion batteries (LIBs) are now the leading energy storage systems, but the insufficiency, fast consumption, and high coast of lithium resources concern on its sustainability [1, 2]. Sodium-ion batteries (SIBs) are appearing as alternative energy storage device for replacing lithium-ion batteries because of the Li-like electrochemical behaviour and the crystal abundance of sodium [3, 4]. Over the past decade, graphite has been considered as a state-of-the-art anode material for LIBs. Unfortunately, it is an ineffective host for Na ions, showing the low theoretical capacity because of larger Na-ion radius [5, 6]. It is pivotal problem to develop high-performance electrode materials and stimulate the commercial development of the high-efficiency and low-price devices based on SIBs and LIBs systems [7–10].

Two-dimensional (2*D*) layer-structured metal-sulphide materials have a great potential as anode materials for SIBs owing to their inherent structure-related properties in physical, chemical, electronic as well as optical aspects [11–19]. Among these materials, SnS_2 can have high theoretical capacity and good reversibility due to its overwhelming merits such as large interlayer spacing and high reversible-conversion efficiency [20–27].

2. METHODS AND MODELS OF CALCULATION

The results of the study of the properties of Na and Li atoms intercalated into the battery anode made on the SnS_2 base were obtained using the author's program code [28], which is based on the methods of the functional of electron density and *ab initio* pseudopotential [29–35].

To reproduce the material of the battery anode for the accumula-

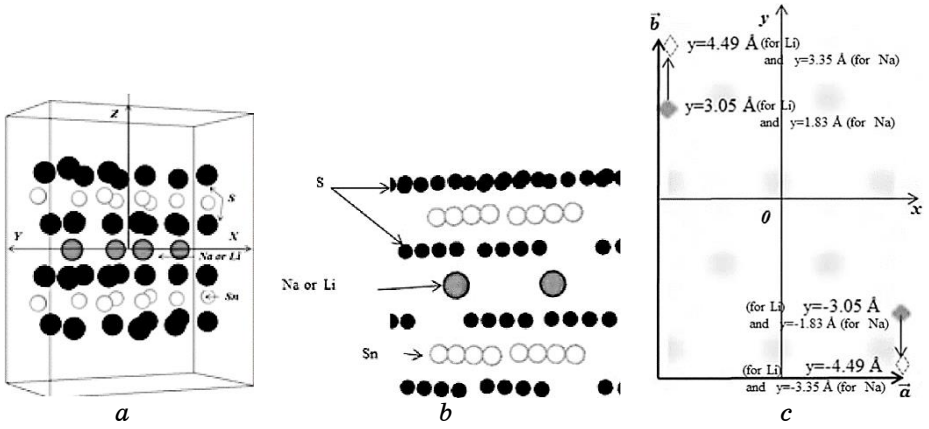

Fig. 1. The direction of migration of the Na or Li atoms from each other into the interlayer of SnS_2 layer within the cell (the view of a primitive cell with an atom basis) (*a*); the fragment of an infinite SnS_2 film with the Na or Li atoms intercalated in its interlayer space (*b*); the cross section of the cell at $c/2$ level with indication of the locus of migration of the Na or Li atoms in the SnS_2 interlayer (*c*).

tion of the Na and Li atoms in the form of two endless monolayers SnS_2 (Fig. 1, *a*), the artificial orthorhombic-type superlattice was created ($a \neq b \neq c$, $\alpha = \beta = \gamma = 90°$); the object at issue is determined by means of parameters of the superlattice and the atom basis. For the simulation of film structure, the lattice cell parameters in the directions of the **a** and **b** crystallographic axes modelled the infinite nanostructured SnS_2 film (Fig. 1, *b*); in a plane perpendicular to the surface, the ***c*** crystallographic axis was chosen, so that the translationally located films would not influence one another. The atom basis of a primitive cell consisted of 8 S atoms and 16 Sn atoms. In the SnS_2 interlayer space, it could be arranged from 0 to 16 Li atoms per cell. Li atoms were placed according their location in a solid state at low temperatures.

3. RESULTS AND DISCUSSION

The spatial distributions of the valence-electrons' density and their sections were obtained (Fig. 2); the total energy of the atom system is plotted in Fig. 3; the energy barriers for migration of the Na [32] and Li [33] atoms in the battery anode made of SnS_2 are presented in Fig. 4. The calculated results were obtained for the degrees of filling of the SnS_2 layer by metal atoms from 12.5% to 100%.

Algorithm for calculating the energy barriers for migration of the Na and Li atoms was such that, for each atomic configuration

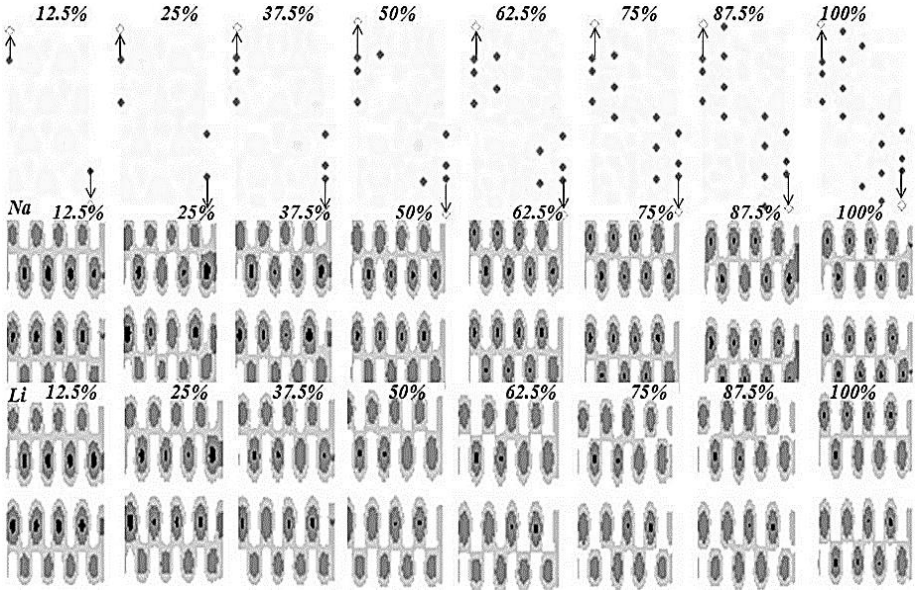

Fig. 2. The (110) cross sections of the spatial distributions of the valence-electrons' density for the filling of the nanostructured SnS_2 interlayers with the Na (top row) and Li (bottom row) atoms at the fullness degrees of 12.5%, 25%, 37.5%, 50%, 62.5%, 75%, 87.5%, 100% from left to right.

corresponding to the elementary step of spatial migration (Fig. 1, *c* (top row)), the total energy was calculated by means of formula:

$$\frac{E_{\text{total}}}{\Omega} = \sum_{\mathbf{k},\mathbf{G},i} \left|b_i(\mathbf{k}+\mathbf{G})\right|^2 \frac{\hbar^2 \left|\mathbf{k}+\mathbf{G}\right|^2}{2m} + \frac{4\pi e^2}{2} \sum_{\mathbf{G}\neq\mathbf{0}}{}' \frac{\left|\rho(\mathbf{G})\right|^2}{\left|\mathbf{G}\right|^2} + \sum_{\mathbf{G}} \varepsilon_{\text{xc}}(\mathbf{G})\rho^*(\mathbf{G}) +$$
$$+ \sum_{\mathbf{k},\mathbf{G},\mathbf{G}',i,l,s} S_s(\mathbf{G}-\mathbf{G}')\Delta V_{l,s}^{NL}(\mathbf{k}+\mathbf{G},\mathbf{k}+\mathbf{G}')b_i(\mathbf{k}+\mathbf{G})b_i^*(\mathbf{k}+\mathbf{G}') + \qquad (1)$$
$$+ \sum_{\mathbf{G},s}{}' S_s(\mathbf{G})V_S^L(\mathbf{G})\rho^*(\mathbf{G}) + \left\{\sum_s \alpha_s\right\}\left[\Omega^{-1}\sum_s Z_s\right] + \Omega^{-1}\gamma_{\text{Ewald}},$$

thus, generating the energy relief along the migration trajectory of the Na and Li atoms. Here, **k** is the vector within the first Brillouin zone, **G** is the vector of the reciprocal lattice, $b_i(\mathbf{k}+\mathbf{G})$ is the coefficient of the expansion of the wave function, i enumerates occupied states for a certain **k**, $\rho(\mathbf{G})$ is the coefficient of decay of the valence-electrons' density, s enumerates atoms in an elementary unit cell, $S_s(\mathbf{G})$ is a structural factor, V_s^L is a local (l-independent) spherically symmetric pseudopotential, l denotes the quantum orbital number, $V_{l,s}^{NL}$ is a nonlocal (l-dependent) additive to V_s^L, Z_s is an ion charge, γ_{Ewald} is the Madelung energy of point ions.

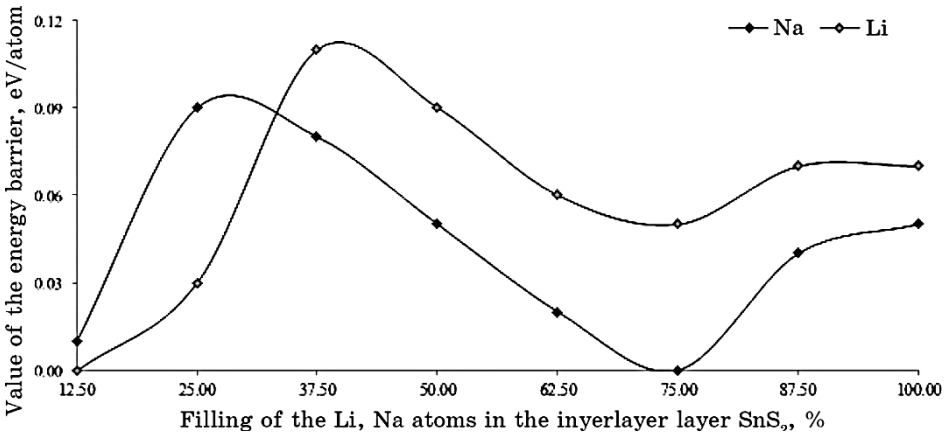

Fig. 3. Graph of dependence of the energy barrier on the filling of Na and Li atoms in the interlayer nanostructured SnS_2 layers.

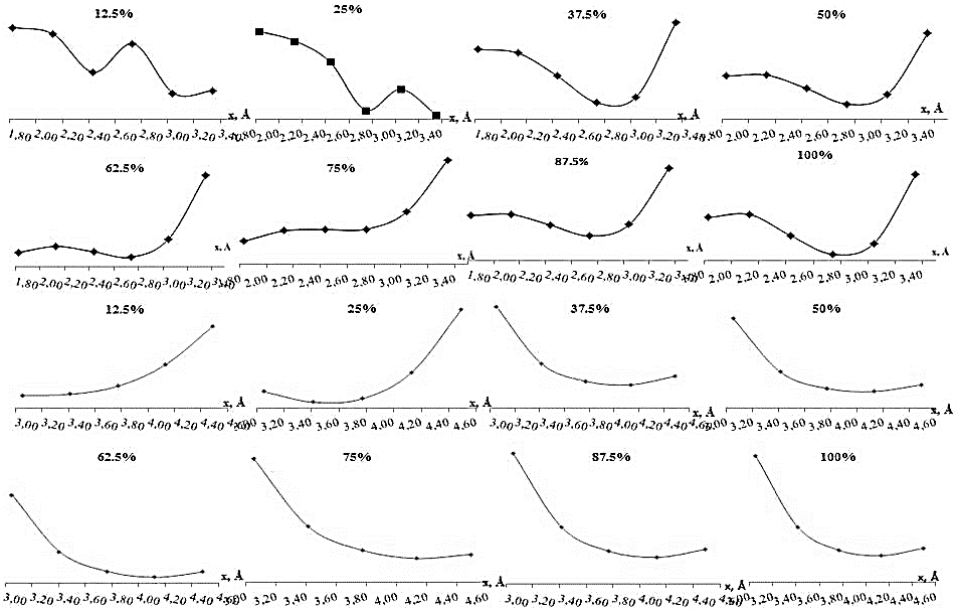

Fig. 4. Graph of the migration energy reliefs of Na (top row) and Li (bottom row) atoms at degrees of filling of the SnS_2 layer from 12.5 to 100%.

The length of migration trajectory was of 1.44 Å and 1.52 Å, and a displacement step was 0.36 Å and 0.30 Å for Na and Li, respectively. The reference level of energy on the energy relief graphs was taken to be equal to –391.02 eV/atom, *i.e.*, the value of the total energy of the system at zero filling of the SnS_2 layer. The total energy

of the system is increased with the number of the Na and Li atoms in the SnS_2 layer.

Figure 4 shows the energy curves during the migration of two Na atoms (two top graphs) and Li atoms (two bottom graphs) from each other at different filling of the interlayer with the Na and Li atoms, respectively. It can be seen that the movement of the intercalated Na and Li atoms into the SnS_2 interlayer space was accompanied by the overcoming of energy barriers, the magnitudes of which are dependent on the degree of filling of the SnS_2 layer with metal atoms. The barrier value was determined by the difference between the minimum and maximum values on the energy-relief curve. Thus, the migration energy reliefs for the Na and Li atoms have one appearance when the SnS_2 layer was filled up to 12.5% and 25%, and the other appearance is at a percentage of 37.5% or more (Fig. 4). However, when the SnS_2 layer was filled with 12.5–25% Na atoms, the energy reliefs have two highs and lows, while the same energy barrier was observed at the same filling with Li atoms. From these figures, it can be seen that, at the final step of the trajectory, the motion of Na atoms, when the interlayer SnS_2 is filled with 37.5% or more, the total energy of the system increases rapidly, and on the contrary, this energy for Li atoms decreases.

Figure 3 shows that, for the intercalated atoms of both Na and Li in the interlayer space of the battery anode made of SnS_2, there is an optimal filling of the layer with atoms of 75%, when the atoms in motion practically did not spend energy.

The presence of significant energy barriers on the migration trajectory of the Na and Li atoms in the SnS_2 layer up to 37.5% can be explained by the interaction of the Na and Li atoms with the SnS_2 surface layer consisting of sulphur atoms. The presence of such interaction was confirmed by the appearance of cross sections of the spatial distributions of the valence electrons' density for the indicated degrees of filling (Fig. 2). The intense grey colour shows that, in the region of sulphur atoms close to the Na and Li atoms, there was a higher density of valence electrons. Starting from an interlayer fill of 62.5%, the density of valence electrons attached to SnS_2 layers no longer had such features.

4. CONCLUSION

By means of the methods of electron-density functional and pseudopotential of the first principles, using the author's program code, we calculated the spatial distributions of the valence electrons' density and their intersections, energy barriers for migration of the Na and Li atoms in the interlayer of the battery anode made of nanostructured SnS_2 films containing 12.5%–100% intercalated atoms.

It was found that, as the number of metal atoms is increased in the SnS_2 interlayer space, the total energy of the atom system is increased too. The movement of intercalated metal atoms was accompanied by the overcoming of energy barriers, the magnitude of which depends on the degree of filling of the nanostructured SnS_2 layer with metal atoms. It was found that there is an optimal situation characterized by the lowest energy losses, when the SnS_2 layer is filled with the Na and Li atoms in percentage of 75%.

The processes, which took place inside the SnS_2 layer during the migration of the intercalated Na and Li atoms, were determined by the interactions of the metal atoms with each other filling the layers, as well as by the interactions of the Na and Li atoms with the nanostructured SnS_2 surface sulphur layer.

From the analysis of energy barriers for the migration of Na and Li atoms, it can be concluded that the SnS_2-based anode is better to be filled with Na atoms. After all, the total energy of the system at the intercalation of Na atoms in the nanostructured SnS_2 layer is less than at the intercalation of Li atoms.

REFERENCES

1. R. Schmuch, R. Wagner, G. Hörpel, T. Placke, and M. Winter, *Natl. Energy*, **3**, No. 4: 267 (2018); https://doi.org/10.1038/s41560-018-0107-2
2. L. Liu, X. Yin, J. Li, S. Wang, Y. Guo, and L. Wan, *Adv. Mater.*, **30**, No. 10: 1706216 (2018); https://doi.org/10.1002/adma.201706216
3. H. Pan, Y. Hu, and L. Chen, *Energy & Environ. Sci.*, **6**: 2338 (2013); https://doi.org/10.1039/C3EE40847G
4. W. Tang, X. Wang, D. Xie, X. Xia, C. Gu, and J. Tu, *J. Mater. Chem. A*, **6**: 18318 (2018); https://doi.org/10.1039/C8TA06905K
5. F. Yang, Z. Zhang, Y. Han, K. Du, Y. Lai, and J. Li, *Electrochim. Acta*, **178**: 871 (2015); https://doi.org/10.1016/j.electacta.2015.08.051
6. A. Metrot, D. Guerard, D. Billaud, and A. Herold, *Synthetic Metals*, **1**: 363 (1980); https://doi.org/10.1016/0379-6779(80)90071-5
7. P. Lu, Y. Sun, H. Xiang, X. Liang, and Y. Yu, *Adv. Energy Mater.*, **8**: 1702434 (2018); https://doi.org/10.1002/aenm.201702434
8. H. Pan, Y. Hu, and L. Chen, *Energy Environ. Sci.*, **6**: 2338 (2013); https://doi.org/10.1039/C3EE40847G
9. Y. Sun, X. Liang, H. Xiang, and Y. Yu, *Chin. Chem. Lett.*, **28**: 2251 (2017).
10. L. Wang, L. Yu, X. Wang, M. Srinivasan, and Z. Xu, *Mater. Chem.*, **3**: 9353 (2015); https://doi.org/10.1039/C4TA06467D
11. F. Cheng, J. Chen, and X. Gou, *Adv. Mat.*, **18**: 2561 (2006); https://doi.org/10.1002/adma.200600912
12. E. Cho, K. Song, M. H. Park, K.-W. Nam, and Y.-M. Kang, *Small*, **12**, Iss. 18: 2510 (2016); https://doi.org/10.1002/smll.201503168
13. S. Fleischmann, T. S. Dörr, A. Frank, S. W. Hieke, D. Doblas-Jimenez, C. Scheu, P. W. de Oliveira, T. Kraus, and V. Presser, *Batteries & Supercaps*, Iss. 2: 668 (2019); https://doi.org/10.1002/batt.201900035

14. H. Liu, H. Guo, B. Liu, M. Liang, K. Adair, and X. Sun, *Adv. Functional Mater.*, **28**: 1707480 (2018); https://doi.org/10.1002/adfm.201707480
15. H. Liu, D. Su, R. Zhou, B. Sun, G. Wang, and S. Qiao, *Adv. Energy Mater.*, **2**, No. 8: 970 (2012); https://doi.org/10.1002/aenm.201200087
16. L. Shi, D. Li, P. Yao, J. Yu, C. Li, B. Yang, C. Zhu, and J. Xu, *Small*, **14**, Iss. 41: 1870187 (2018); https://doi.org/10.1002/smll.201870187
17. D. Su, S. Dou, and G. Wang, *Chem. Commun.*, **50**, No. 32: 4192-5 (2014); https://doi.org/10.1039/C4CC00840E
18. G. Wang, J. Zhang, S. Yang, F. Wang, X. Zhuang, K. Müllen, and X. Feng, *Adv. Energy Mater.*, **8**, No. 8: 1702254 (2018); https://doi.org/10.1002/aenm.201702254
19. S. Wang, F. Gong, S. Yang, J. Liao, M. Wu, Z. Xu, C. Chen, X. Yang, F. Zhao, B. Wang, Y. Wang, and X. Sun, *Adv. Functional Mater.*, **28**, No. 34: 1801806 (2018); https://doi.org/10.1002/adfm.201801806
20. S. Chu, Y. Cui, and N. Liu, *Nat. Mater.*, **16**: 16 (2017); https://doi.org/10.1038/nmat4834
21. Z. Li, J. Ding, and D. Mitlin, *Acc. Chem. Res.*, **16**: 1657 (2015); https://doi.org/10.1021/acs.accounts.5b0014
22. C. Grey and J. Tarascon, *Nat. Mater.*, **16**: 45 (2017); https://doi.org/10.1038/nmat4777
23. X. Ou, L. Cao, X. Liang, F. Zheng, H.-S. Zheng, X. Yang, J.-H. Wang, C. Yang, and M. Liu, *ACS Nano*, **13**, No. 3: 3666 (2019); https://doi.org/10.1021/acsnano.9b00375
24. B. Qu, C. Ma, G. Ji, C. Xu, J. Xu, Y. Meng, T. Wang, and J. Lee, *Adv. Mater.*, **26**, No. 23: 3854 (2014); https://doi.org/10.1002/adma.201306314
25. C. Zhai, N. Du, and H. Yang, *Chem. Commun.*, **47**: 1270 (2011); https://doi.org/10.1039/C0C03023F
26. Y. Zhang, P. Zhu, L. Huang, J. Xie, S. Zhang, G. Cao, and X. Zhao, *Adv. Functional Mater.*, **25**: 481 (2015); https://doi.org/10.1002/adfm.201402833
27. Y. Zhao, B. Guo, Q. Yao, J. Li, J. Zhang, K. Hou, and L. Guan, *Nanoscale*, **10**, No. 17: 7999 (2018); https://doi.org/10.1039/c8nr01783b
28. *Ab initio Calculation [Electronic course]: Internet-portal Access mode*: http://sites.google.com/a/kdpu.edu.ua/calculationphysics/ - Screen title
29. W. Kohn and L. Sham, *Phys. Rev.*, **140**, No. 4A: A1133 (1965); https://doi.org/10.1103/PhysRev.140.A1133
30. G. Makov, R. Shah, and M. Payne, *Phys. Rev.*, **B53**: 15513 (1996); https://doi.org/10.1103/PhysRevB.53.15513
31. G. Bachelet, D. Hamann, and M. Schlüter, *Phys. Rev.*, **B26**: 4199 (1982); https://doi.org/10.1103/PhysRevB.26.4199
32. R. Balabai and Yu. Prikhozha, *J. Phys. Stud.*, **23**, No. 3: 3703-1 (2019) (in Ukrainian); https://doi.org/10.30970/jps.23.3703
33. R. Balabai and Yu. Prikhozha, *Phys. Chem. Solid State*, **20**, No. 2: 120 (2019) (in Ukrainian); https://doi.org/10.15330/pcss.20.2.120-126
34. R. Balabai, D. Kravtsova, P. Merzlykin, and Yu. Prihozhaya, *J. Nanophotonics*, **12**, No. 3: 036003 (2018) (in Ukrainian); https://doi.org/10.1117/1.JNP.12.036003
35. R. M. Balabai, Yu. Prikhozha, and O. H. Tadeusz, *Sensor Electronics and Microsystem Technologies*, **6**, No. 1: 50 (2019) (in Ukrainian); http://dx.doi.org/10.18524/1815-7459.2019.1.159487